*medicina*

MDPI

*Article*

# Assessing Liver Fibrosis Using 2D-SWE Liver Ultrasound Elastography and Dynamic Liver Scintigraphy with 99mTc-mebrofenin: A Comparative Prospective Single-Center Study

**Donatas Jocius [1,*], Donatas Vajauskas [2], Artūras Samuilis [1], Kipras Mikelis [1], Skirmante Jokubauskiene [3], Kestutis Strupas [4] and Algirdas E. Tamosiunas [1]**

[1] Department of Radiology, Nuclear Medicine and Medical Physics, Institute of Biomedical Sciences, Faculty of Medicine, Vilnius University, LT-01513 Vilnius, Lithuania
[2] Department of Radiology, Medical Academy, Lithuanian University of Health Science Kauno Klinikos, LT-44307 Kaunas, Lithuania
[3] National Center of Pathology, LT-01513 Vilnius, Lithuania
[4] Clinic of Gastroenterology, Nephro-Urology and Surgery, Institute of Clinical Medicine, Faculty of Medicine, Vilnius University, LT-01513 Vilnius, Lithuania
* Correspondence: jocius.donatas@gmail.com

**Abstract:** *Background and Objectives:* Many quantitative imaging modalities are available that quantify chronic liver disease, although only a few of them are included in clinical guidelines. Many more imaging options are still competing to find their place in the area of diagnosing chronic liver disease. We report our first prospective single-center study evaluating different imaging modalities that stratify viral hepatitis-associated liver fibrosis in a treatment-naïve patient group. *Materials and Methods:* The aim of our study is to compare and to combine already employed 2D shear wave elastography (2D-SWE) with dynamic liver scintigraphy with 99mTc-mebrofenin in chronic viral hepatitis patients for the staging of liver fibrosis. *Results:* Seventy-two patients were enrolled in the study. We found that both 2D-SWE ultrasound imaging, with dynamic liver scintigraphy with 99mTc-mebrofenin are able to stratify CLD patients into different liver fibrosis categories based on histological examination findings. We did not find any statistically significant difference between these imaging options, which means that dynamic liver scintigraphy with 99mTc-mebrofenin is not an inferior imaging technique. A combination of these imaging modalities showed increased accuracy in the non-invasive staging of liver cirrhosis. *Conclusions:* Our study presents that 2D-SWE and dynamic liver scintigraphy with 99mTc-mebrofenin could be used for staging liver fibrosis, both in singular application and in a combined way, adding a potential supplementary value that represents different aspects of liver fibrosis in CLD.

**Keywords:** chronic liver disease; liver fibrosis; ultrasound elastography; dynamic liver scintigraphy; 99mTc-mebrofenin



**Citation:** Jocius, D.; Vajauskas, D.; Samuilis, A.; Mikelis, K.; Jokubauskiene, S.; Strupas, K.; Tamosiunas, A.E. Assessing Liver Fibrosis Using 2D-SWE Liver Ultrasound Elastography and Dynamic Liver Scintigraphy with 99mTc-mebrofenin: A Comparative Prospective Single-Center Study. *Medicina* **2023**, *59*, 479. https://doi.org/10.3390/medicina59030479

Academic Editor: Hirayuki Enomoto

Received: 12 January 2023
Revised: 17 February 2023
Accepted: 23 February 2023
Published: 28 February 2023



## 1. Introduction

Chronic liver disease (CLD) is a hallmark result of long-standing liver injury, with hepatitis virus infections, mainly hepatitis B and hepatitis C, being one of the leading causes and being responsible for almost 40% of CLD worldwide [1,2]. Other causes include NAFLD/NASH (nonalcoholic fatty liver disease/nonalcoholic steatohepatitis), alcohol, primary biliary cirrhosis, primary sclerosing cholangitis, α1 antitrypsin deficiency, Wilson's disease, and autoimmune hepatitis [2]. Although there is a general trend of decreasing CLD mortality rates in the world, inequality between different regions is present [3]. In addition, the World Health Organization has stated that viral hepatitis infections have caused over one million deaths in 2019 [4].

*Aim*

The aim of this prospective, non-randomized study is to compare already employed 2D-SWE ultrasound imaging with dynamic liver scintigraphy with 99mTc-mebrofenin in chronic viral hepatitis patients for the staging of liver fibrosis before initiating primary treatment. The histological evaluation of the hepatic tissue was used as a reference.

Multiple pathological factors affect the liver, with damage commonly resulting in liver fibrosis [5]. In general, pathogenic factors affecting the liver lead to the death of hepatocytes and the infiltration of immunogenic cells. Inflammatory alteration turns hepatic stellate cells into myofibroblasts—key cells for the production of collagen [6]. In the short term, this process is balanced and works to repair damaged liver tissue, while in chronic disease, the balance is disrupted and leads to an overproduction of the extracellular matrix [7,8].

In the early stages, liver fibrosis remains clinically silent most of the time, but on the other hand, as fibrosis progresses to its advanced stages, it alters liver function, leading to hepatic insufficiency and liver cirrhosis [9]. These alterations cause many devastating and life-threatening complications—portal hypertension and portosystemic varices, splenomegaly, ascites and spontaneous bacterial peritonitis, hepatorenal, hepatopulmonary syndromes, coagulopathy, bone-related diseases (osteopenia and osteoporosis), hematologic abnormalities, and liver cancer [10].

Clinical signs and symptoms such as jaundice, splenomegaly, ascites, gynecomastia, and others may not necessarily approach as the disease progresses [11]. Many patients without any clinical signs of liver damage may have been diagnosed with liver fibrosis via laboratory assays, imaging, or instrumental tests [12].

Once the diagnosis of CLD is present, a quantitative assessment of liver parenchyma is needed to stratify the risk of potential complications, deciding on the time and regime of treatment, and as a basic point for longitudinal follow-up [13,14].

Liver biopsy is historically the "golden" standard for directly assessing liver fibrosis stage, inflammatory activity, steatosis level, biliary disease, and other overlapping syndromes, and it is still incorporated into clinical guidelines [13,15]. On the other hand, liver biopsies are prone to many drawbacks, including their invasiveness, small sampling size, high interobserver and intraobserver variability, a limited availability for longitudinal follow-up, and the relatively high price and low accuracy [13,15].

At present, several imaging techniques are employed to quantitate diffuse hepatic tissue changes in patients with CLD. One of the most often used are ultrasound elastography with its several types, including transient elastography (TE), point shear wave elastography (pSWE), real time 2D shear wave elastography (2D-SWE), and to a lesser extent, magnetic resonance elastography (MRE) with several different sequences [16–19]. Nevertheless, both imaging and clinical guidelines suggest elastography as a method for ruling out advanced liver fibrosis rather than diagnosing it [15,16,20–23]. In addition, variable cutoff values measured with different vendor machines may overlap; thus, recommendations usually advise against using it in separating the exact fibrosis stage [24].

Computed tomography was also tested in quantitating chronic liver disease with several approaches, including liver surface nodularity or the liver segmental volume ratio, although software availability and the accuracy of these methods in the early stages of the disease are limited [18,25–28].

All of the abovementioned imaging techniques depict mechanical changes within the liver, which are associated with the amount of fibrotic tissue. Altered liver structural composition changes the liver's mechanical properties, namely, elasticity and viscosity [29–31]. Measuring these mechanical deviations is a non-direct assessment of deteriorating liver function, and it is also related to several pitfalls and physiological states [13]. Liver stiffness measured via both USE and MRE could be elevated when liver inflammation, infiltrative liver disease, congestive heart disease, cholestasis, food ingestion, and physical activity are present without any liver fibrosis [15,24].

During the course of CLD, the advancing fibrosis makes the liver undergo structural changes, together with its functional deterioration [5]. To date, only scarce literature can be

found on the role of functional imaging in CLD [32,33]. Nevertheless, functional imaging with several different nuclear medicine tracers was proven to represent liver function, predicting future remnant liver in major liver surgery [34–38].

Moreover, dynamic liver scintigraphy with 99mTc-mebrofenin showed to be as accurate as Gd-EOB-DTPA enhanced magnetic resonance imaging (MRI) when evaluating changes in liver function after portal vein embolization [36].

Our recently published data prove that dynamic liver scintigraphy with 99mTc-mebrofenin can stratify patients with CLD. Many scintigraphy parameters were found to be significant when predicting different liver fibrosis stages. Of all the calculated parameters, tracer retention in the liver and liver clearance were the most accurate ones [39]. Nevertheless, this modality still needs to be compared with the already established one.

## 2. Materials and Methods

During the period of August 2018 to January 2020, we prospectively invited patients who were referred to our center for a liver biopsy procedure as initial staging, to participate in this study and to undergo both imaging procedures and a liver biopsy. All agreeing participants have provided their informed consent. The study was approved by the local biomedical ethics committee (Vilnius Regional Biomedical Research Ethics Committee, Reg. No 158200-16-877-386), and the study was conducted according to the principles of the Helsinki Declaration.

Imaging procedures (2D-SWE and dynamic liver scintigraphy with 99mTc-mebrofenin) were performed on the same day. Patients were instructed to fast for at least 4 h before the procedure, and were advised against consuming coffee or energy drinks, or smoking. The imaging took place after a rest period of 10–15 min.

Liver ultrasound elastography 2D-SWE (GE Logiq E9 system, GE Healthcare, Wauwatosa, WI, USA) was performed using the convex probe in a supine position with the right arm elevated above the head. Measurements were performed in the right liver lobe, avoiding major blood vessels, and at least 1 cm away from liver capsule. Ten measurements were performed in each patient, and the results were expressed in kPa. Measurements within the interquartile range to median range (IQR/M) of less than 30% were accepted as being valid. The 2D-SWE imaging protocol was set according to Barr et al. [24]

Subsequently, on the same day, all patients underwent dynamic liver scintigraphy with 99mTc-mebrofenin on the GE Infinia Hawkeye dual head SPECT/CT gamma camera (GE Healthcare, Milwaukee, WI). Dynamic planar imaging was performed using low energy high resolution (LEHR) collimators (energy window 130–150 keV, matrix 64 × 64). The patient was placed in the supine position, and imaging was set immediately after an intravenous bolus injection of 99mTc-mebrofenin (Bridatec, GE Healthcare; median activity 205.5 MBq (SD ±14.15 MBq)) and continued for 30 min. The imaging protocol was adjusted according to Rassam et al. [38].

Data gathered were reconstructed using a GE Xeleris 2 workstation (General Electric Healthcare, Milwaukee, WI, USA). The geometric mean (Gmean) dataset was used for region of interest (ROI) placement.

Despite gathering the data of many dynamic liver scintigraphy parameters, in this comparison study, we used the liver clearance (LCL) of the right liver lobe, representing the amount of tracer extracted by the liver from the blood to the biliary system (a direct measurement of liver function). LCL was calculated according to Ekman et al. [40]. The LCL measurement was corrected for body surface area (BSA) and liver area (LA) to acquire a universal, patient-, and ROI size-independent result, and this was expressed in $\%/min/m^2/dm^2$. The ROI of LCL was drawn on the right liver lobe, excluding the major biliary ducts and gall bladder.

Both imaging procedures were performed by the same investigator (D.J.) to maximize sampling of the same liver area, and to exclude interobserver variability.

Participants underwent a liver biopsy within two weeks after imaging studies. Liver biopsy procedures were performed using an 18-gauge biopsy needle to sample 2 or 3 biopsy

cores in the right liver lobe to obtain a representative sample of at least 3 cm of total length. A histological examination was performed by an experienced pathologist (S.J.). METAVIR, hepatitis activity index (HAI) according to Ishak, and liver steatosis scores were evaluated.

The data were analyzed using Microsoft Excel (Microsoft Corporation, 2018), IBM SPSS Statistics (Version 25.0. Armonk, NY, USA: IBM Corp.), MedCalc Statistical Software (version 20.116. MedCalc Software bv, Ostend, Belgium), and Rstudio (version 2022.07.2. RStudio Team. RStudio: Integrated Development Environment for R. Boston, MA, USA).

All variables were tested for normality using the Shapiro–Wilk test; statistical tests were selected accordingly, and data were expressed as mean and standard error when normal data distribution was present, or in median and range if normal data distribution was not found.

We looked for associations between the fibrosis score from the core needle biopsy sample, using 2D-SWE and LCL scintigraphy parameters. Student's t-test was used to find differences between two groups of variables with normal distribution, and the Mann–Whitney U test, for non-parametric continuous variables. For differences between three or more groups, a one-way analysis of variance (ANOVA) and the Kruskal–Wallis H test were used. Pearson's correlation test and Spearman's rank-order correlation coefficient were used to find correlations between continuous variables. A binomial logistic regression model was used to investigate whether a combination of independent variables predicted a probability of fibrosis stage. An R program, Compbdt, was used to compare sensitivity and specificity between tests for liver fibrosis (2D-SWE, LCL, or a regression model). A MedCalc function, Comparison of ROC curves, with the method of DeLong et al., was used to compare areas under the curve of these tests, and the Youden Index was used to set the threshold values [41,42]. The significance level was set at 0.05.

We calculated the sample size needed to achieve the desired statistical power for our study. For SWE, we used an estimate of AUC to be approximately 0.9, and predicted a 15 percent difference between the SWE and the scintigraphy measurements AUC. Then, using the estimation from Hajian-Tilaki, we calculated that a sample size of 70 patients was needed to achieve a 95% confidence level and 80% power [43].

## 3. Results

### *3.1. Patients*

One hundred and six patients were invited to participate in the study, and 72 of them agreed to participate and signed informed consent forms. Imaging studies of both 2D-SWE and dynamic liver scintigraphy with 99mTc-mebrofenin were performed in all patients, and only one liver biopsy procedure was skipped due to an unrelated urgency precluding an invasive procedure (patient data was excluded from further analysis).

The mean patient age was 45 years (a range of 18–80 years). Sixty-eight participants had chronic hepatitis C (HCV), and four had chronic hepatis B (HBV). Nine patients also had a human immunodeficiency virus (HIV) coinfection.

The mean body mass was 81.89 kg (a range of 48–130 kg). The mean body surface area (BSA) (used for correction purposes) was 1.98 $m^2$ (range: 1.45–2.52 $m^2$) (Table 1).

**Table 1.** Demographic data of study population.

| Variable | Value |
|---|---|
| Age (years) | 45 years (SD 13.4) |
| Gender | |
| Male | 45 (62.5%) |
| Female | 27 (37.5%) |
| Weight (kg) | 82.28 kg (SD 17.6) |
| BMI ($kg/m^2$) | 26.5 $kg/m^2$ (17.51–42 $kg/m^2$) |
| BSA ($m^2$) | 1.98 $m^2$ (SD 0.23) |
| Virus type in patient population | |
| HBV | 4 (5%) |
| HCV | 68 (95%) |
| HIV coinfection | 9 (12%) |

BMI—body mass index, BSA—body surface area, HBV—hepatitis B virus, HCV—hepatitis C virus, HIV—human immunodeficiency virus.

All patients included in the study were treatment-naïve.

### *3.2. Histological Examination*

The results of the histological examination are presented in Table 2. One should note that the histological analysis covers all but one patient who skipped a liver biopsy procedure. All of the other patients conceded to liver biopsy, and an analysis of biopsy specimens is available.

**Table 2.** Distribution of liver fibrosis stages in the study population according to pathological examination.

| | F1 | F2 | F3 | F4 |
|---|---|---|---|---|
| METAVIR | 14 (19.4%) | 38 (52.8%) | 12 (16.7%) | 7 (9.7%) |

### *3.3. Imaging Studies*

#### 3.3.1. Ultrasound Elastography: 2D-SWE Findings

The 2D-SWE was completed in all patients. There were no nondiagnostic examinations. The median liver stiffness in the study population was 6.73 kPa (range: 3.47 kPa–48.8 kPa). Liver fibrosis was evaluated via histological examination, patients were divided into four categories, and the liver stiffness median was calculated for each of these four categories (Figure 1).

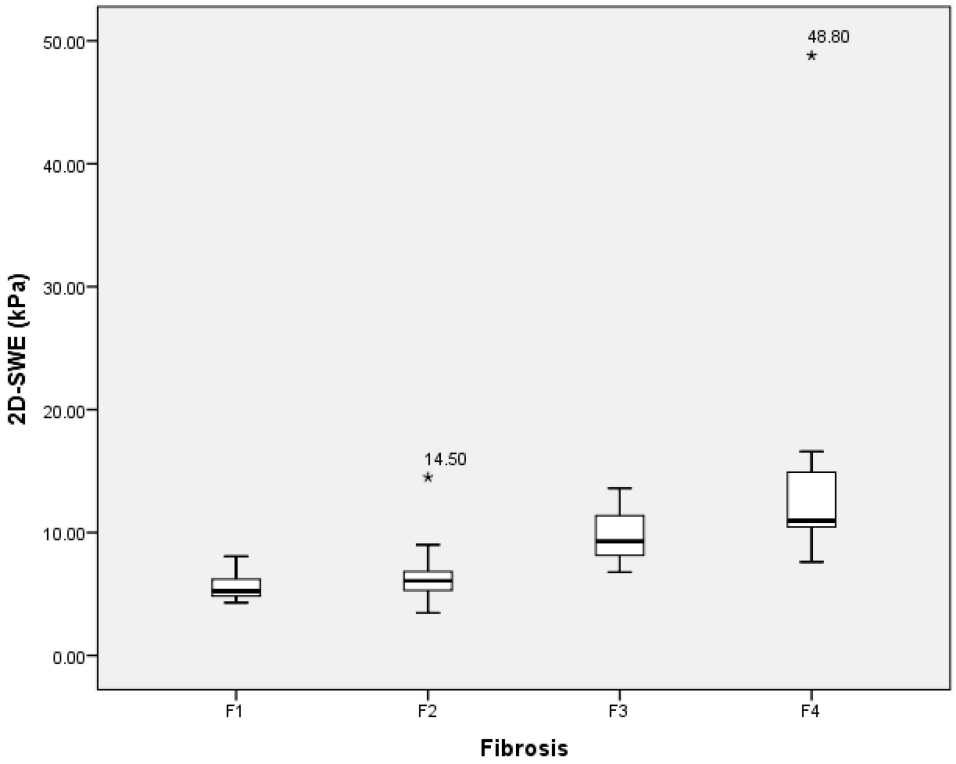


**Figure 1.** Box plot of the liver stiffness median, measured using 2D-SWE in different liver fibrosis categories according to METAVIR score. Median values: F1—5.23 kPa, F2—6.08 kPa, F3—9.28 kPa, and F4—10.97 kPa. 2D-SWE—multidimensional shear wave elastography.

The results of the histological examination were taken as a base value, and by relying on the histology grades of liver fibrosis, we calculated the 2D-SWE threshold values in different liver fibrosis stages (Table 3).

**Table 3.** 2D-SWE threshold values defining different liver fibrosis stages.

| Liver Fibrosis | 2D-SWE Value (kPa) | AUROC | Sensitivity (%) | Specificity (%) |
|---|---|---|---|---|
| F1 vs. F2-F4 | 5.4 kPa | 0.75 | 82% | 65% |
| F1-F2 vs. F3-F4 | 7.16 kPa | 0.93 | 89% | 79% |
| F1-F3 vs. F4 | 9.9 kPa | 0.91 | 85% | 91% |

The 5.4 kPa value differentiated F1 (mild fibrosis) versus F2–F4. A threshold value of 7.16 kPa was set for differentiating F1–F2 versus F3–F4 (significant fibrosis), and a threshold value of 9.9 kPa was set for defining advanced fibrosis (F1–F3 versus F4).

#### 3.3.2. Dynamic Liver Scintigraphy with 99mTc-mebrofenin

The liver clearance of the right lobe was selected because liver biopsies were only performed on the right liver lobe, and also as the only 2D-SWE measurement. The median LCL was 3.73%/min/$m^2$/$dm^2$ (range: 1.49%/min/$m^2$/$dm^2$–9.35%/min/$m^2$/$dm^2$); its results at different liver fibrosis stages are presented in Figure 2.

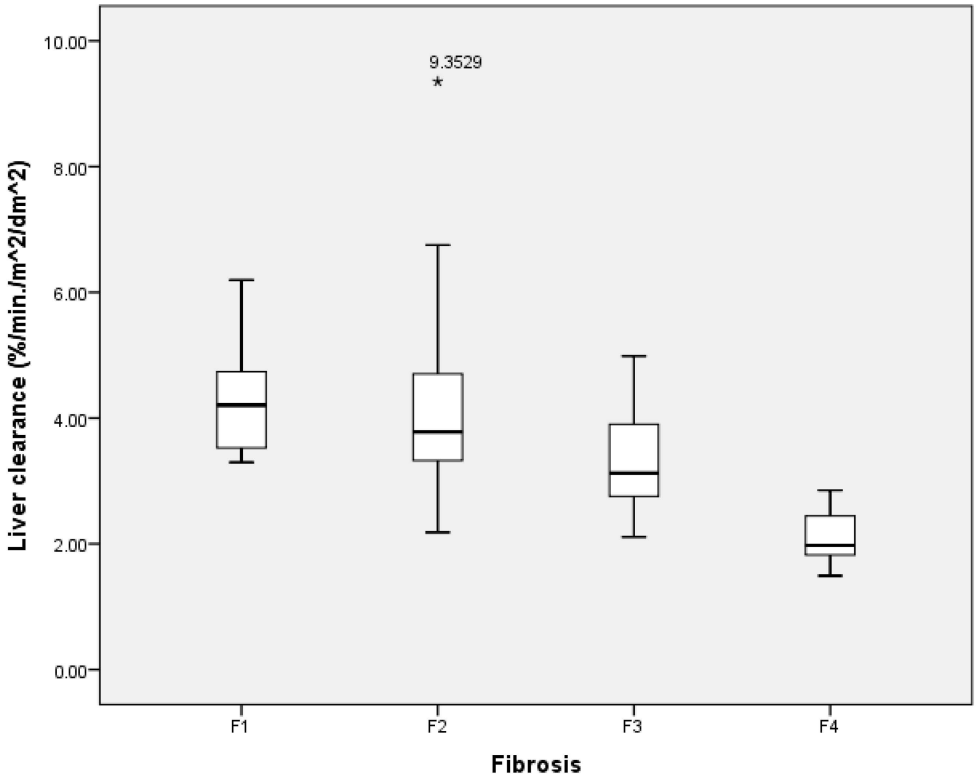


**Figure 2.** Box plot of the liver clearance (LCL) median, measured using dynamic liver scintigraphy with 99mTc-mebrofenin in different liver fibrosis categories according to the METAVIR score. Median values: F1—4.21%/min/$m^2$/$dm^2$; F2—3.78%/min/$m^2$/$dm^2$; F3—3.13%/min/$m^2$/$dm^2$; F4—1.98%/min/$m^2$/$dm^2$.

In general, liver clearance was negatively associated with the liver fibrosis stage—liver clearance decreased as the stage of liver fibrosis increased.

Threshold values for LCL were also calculated by relying on a histological examination of the liver biopsy specimen. The LCL of 3.76%/min/$m^2$/$dm^2$ differentiated F1 versus F2–F4, LCL of 3.29%/min/$m^2$/$dm^2$ clearance differentiated F1–F2 versus F3–F4, and an LCL of 2.85%/min/$m^2$/$dm^2$ was set as a point between F1–F3 and F4. The sensitivities, specificities, and AUROC of each threshold are presented in Table 4.

**Table 4.** Liver clearance threshold values defining different liver fibrosis stages.

| Liver Fibrosis | LCL (%/min/$m^2$/$dm^2$) | AUROC | Sensitivity (%) | Specificity (%) |
|---|---|---|---|---|
| F1 vs. F2–F4 | 3.76 | 0.67 | 71% | 60% |
| F1–F2 vs. F3–F4 | 3.29 | 0.83 | 82% | 74% |
| F1–F3 vs. F4 | 2.85 | 0.96 | 87% | 99% |

#### 3.3.3. Comparison between Imaging Studies

Both 2D-SWE and dynamic liver scintigraphy, with 99mTc-mebrofenin imaging methods, were able to separate different levels of liver fibrosis. A pathology examination of the liver biopsy specimen was used as a reference to compare liver stiffness (measured in kPa) and liver clearance (measured in %/min/$m^2$/$dm^2$) between the two imaging methods.

In defining mild versus advanced liver fibrosis (F1 vs. F2–F4), the sensitivity and specificity of 2D-SWE against dynamic liver scintigraphy with 99mTc-mebrofenin was 82% versus 59%, and 64% versus 71%, respectively. The AUROC was 0.75 for 2D-SWE, and 0.68 for dynamic liver scintigraphy with 99mTc-mebrofenin ($p$ value 0.22) (Figure 3).

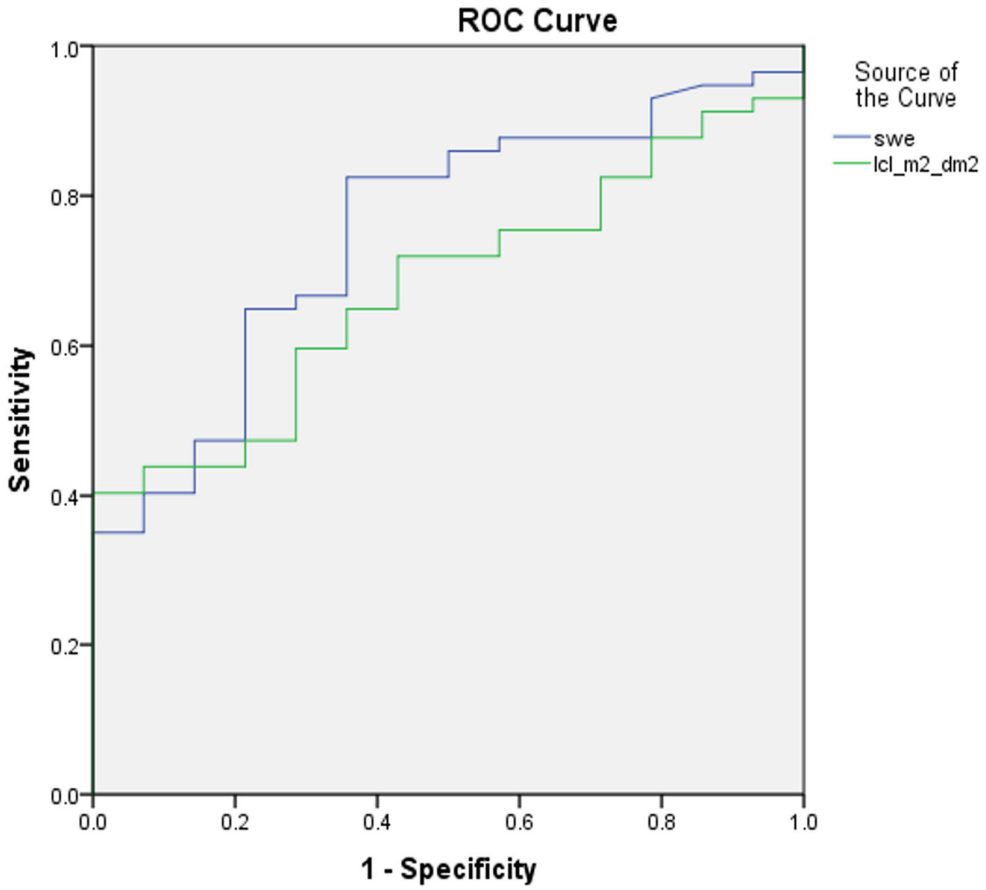


**Figure 3.** ROC curves of 2D-SWE and dynamic liver scintigraphy, with 99mTc-mebrofenin separating mild liver fibrosis; AUROC was 0.75 and 0.68, respectively ($p$ value 0.22). swe—2D-SWE value represented in kPa; lcl_$m^2$_$dm^2$—liver clearance measured in right liver lobe and corrected using BSA and LA.

In separating significant fibrosis (F1–F2 versus F3–F4), 2D-SWE and dynamic liver scintigraphy with 99mTc-mebrofenin showed sensitivities of 94% and 74%, and specificities of 79% and 83%, respectively. The AUROC was 0.93 for 2D-SWE, and 0.83 for dynamic liver scintigraphy, with 99mTc-mebrofenin ($p$ value 0.061) (Figure 4).

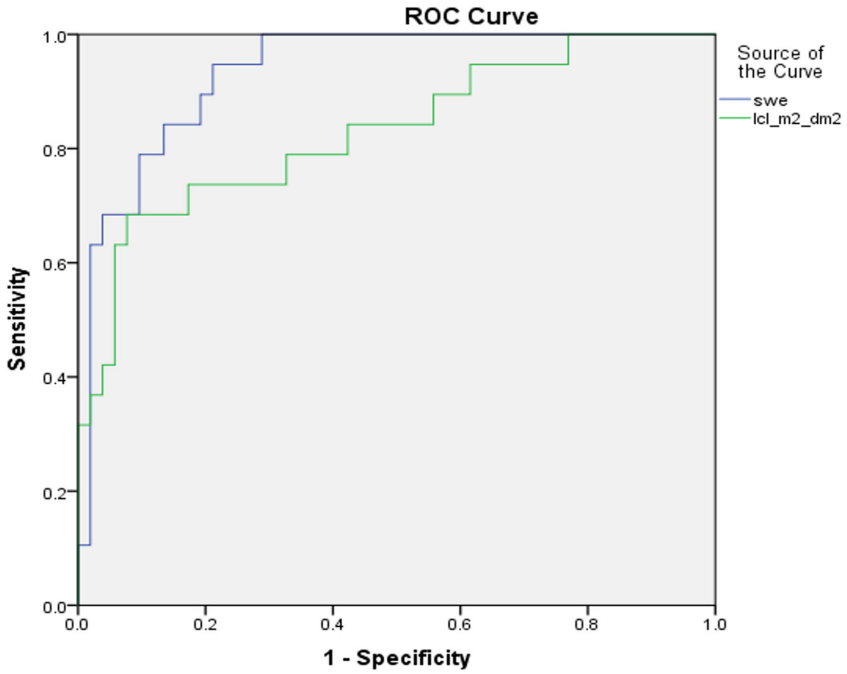


**Figure 4.** ROC curves of 2D-SWE and dynamic liver scintigraphy, with 99mTc-mebrofenin separating significant liver fibrosis; AUROC was 0.93 and 0.83, respectively (*p* value 0.061). swe—2D-SWE value represented in kPa; lcl_$m^2$_$dm^2$—liver clearance measured in the right liver lobe and corrected using BSA and LA.

In separating advanced liver fibrosis/liver cirrhosis (F1–F3 versus F4), we found an 85% sensitivity and 85% specificity for 2D-SWE, and a 90% sensitivity and 87% specificity for dynamic liver scintigraphy with 99mTc-mebrofenin. The AUROC was 0.91 and 0.96, respectively (*p* value 0.33) (Figure 5).

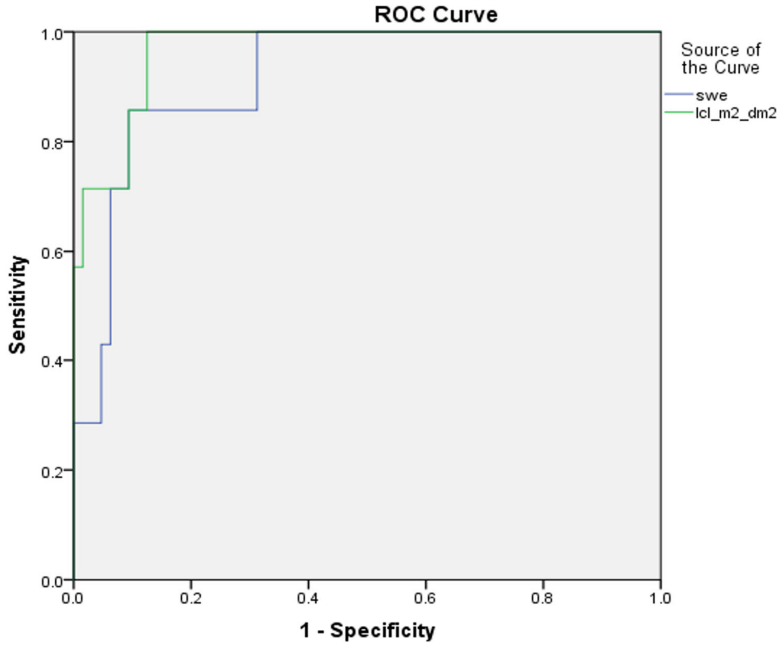


**Figure 5.** ROC curves of 2D-SWE and dynamic liver scintigraphy, with 99mTc-mebrofenin separating liver cirrhosis; AUROC was 0.91 and 0.96, respectively (*p* value 0.33). swe—2D-SWE value, represented in kPa; lcl_$m^2$_$dm^2$—liver clearance measured in right liver lobe and corrected using BSA and LA.

### *3.4. Combination of Two Imaging Tests*

The two imaging methods, 2D-SWE and dynamic liver scintigraphy with 99mTc-mebrofenin, represent in general somewhat different aspects of liver injury. The first one represents the change of the liver's mechanical properties and the increasing amount of fibrotic tissue inside the liver, while the second method reflects alterations in liver function.

As these two methods may in theory be complementary to each other, we combined them in a logistic regression model to see whether this could have any additional value.

Combining liver stiffness with liver clearance in separating mild (F1 versus F2–F4) and significant (F1–F2 versus F3–F4) fibrosis showed no difference in the area under the ROC curve—AUROC remained the same for mild (AUROC 0.75) and significant (AUROC 0.93) fibrosis, before and after the combination. Nonetheless, in liver cirrhosis (F1–F3 versus F4), the combination of the two methods increased imaging accuracy from AUROC 0.91 to 0.98, although the difference was non-significant (*p* value 0.18) (Figure 6).

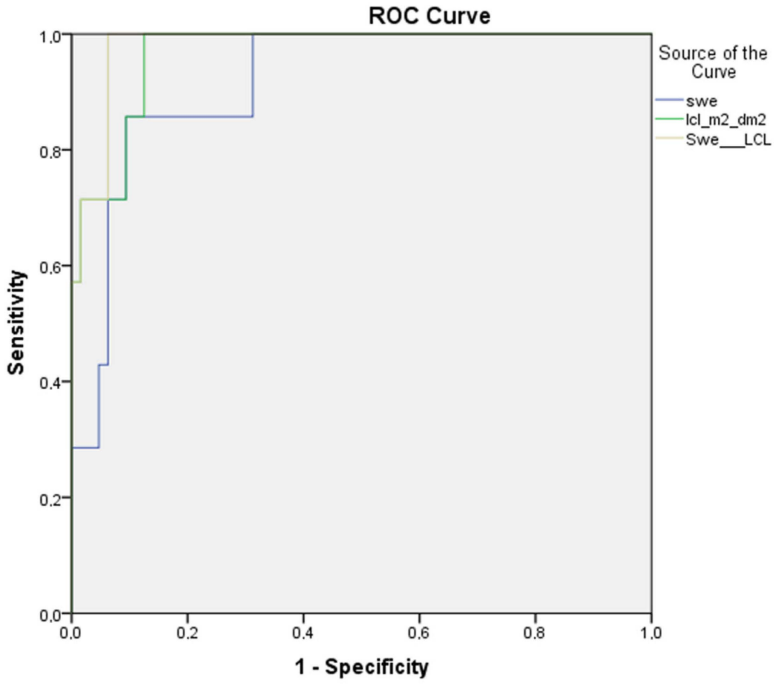


**Figure 6.** Combination of adding 2D-SWE and dynamic liver scintigraphy with 99mTc-mebrofenin together in liver cirrhosis group—the AUROC increased from 0.91 to 0.98. swe—2D-SWE curve before combination; lcl_$m^2$_$dm^2$—liver clearance measured in right liver lobe and corrected using BSA and LA curve before combination; SWE__LCL—combined curve.

## 4. Discussion

Many diagnostic assays have at least some value in diagnosing chronic liver disease, including simple laboratory and panel tests, noninvasive scoring systems, circulatory mRNA assays, several imaging modalities, and liver biopsies. Recently, artificial intelligence was also involved evaluating imaging findings and stratifying liver fibrosis [44–46]. Of note, only a few of these methods are included in clinical guidelines, while others are still competing to find their role in a CLD setting [12,15]

In general, ultrasound and magnetic resonance elastography are approved as valuable imaging tests for quantifying live fibrosis with high accuracy. Moreover, elastography techniques are rather used to rule out significant fibrosis in the low prevalence population. On the other hand, in a high prevalence patient population, guidelines suggest a cut-off to rule in significant fibrosis [15]. It is agreed that defining separate liver fibrosis stages with the presently recommended imaging modalities is not accurate enough, and is probably related to vendor dependency, in addition to physiological and pathological cofactors [16,20,24].

None of the biomarkers are excellent, and even the old "golden" standard—liver biopsy—has many of its own drawbacks related to procedural risk, incorrect evaluation due to sampling errors, a relatively small sample size, and high inter- and intra-observer variability [13,17]. The most widely used ultrasound elastography is also prone to several limitations, including vendor and observer variability, while cofounding pathological and physiological factors can lead to erroneous imaging conclusions [24]. In addition, shear wave elastography itself has several modifications, including transient elastography (TE), point shear wave (pSWE), and 2D shear wave elastography (2D-SWE), also estimating differences by measuring shear wave speed [20].

We note that dynamic liver scintigraphy with 99mTc-mebrofenin imaging has only scarce and indirect evidence in the CLD setting. Nevertheless, dynamic liver scintigraphy with 99mTc- mebrofenin for predicting future remnant liver functional volume is clearly valued and suggested over anatomical volumetry [38,47,48]. It is clear that healthy and abnormal liver parenchyma will have different functional capacities, which may not be present from structural imaging [49,50].

Our group has recently published data indicating that dynamic liver scintigraphy with 99mTc-mebrofenin may separate the different stages of liver fibrosis [39]. Together with other partly related studies using 99mTc-mebrofenin to quantitate liver parenchyma, this has led our group to test this modality in the CLD setting by comparing it with an already employed method—2D-SWE [37,47,49,50].

To our knowledge, this is the first prospective study comparing 2D-SWE imaging with dynamic liver scintigraphy with 99mTc-mebrofenin that uses a histological examination of the liver biopsy specimen as a reference standard in the same group of treatment-naïve patients with chronic viral hepatitis.

Several conclusions could be stated. First, we found that both liver stiffness (measured using 2D-SWE in kPa) and LCL (measured via dynamic liver scintigraphy with 99mTc-mebrofenin in $\%/min/m^2/dm^2$) resemble liver changes at different stages of liver fibrosis. Liver stiffness had a direct positive association with liver fibrosis—liver stiffness increased as fibrosis developed (Figure 7). On the other hand, LCL had a direct negative association to liver fibrosis—it decreased as liver fibrosis developed (Figure 8). The difference in median values between the liver fibrosis stages in each imaging value was significant (Figures 1 and 2).

The 2D-SWE findings reflect the underlying pathological mechanical changes of the liver as an indirect evidence of liver tissue injury. Liver stiffness increases with the increasing amount of fibrotic tissue in the liver parenchyma during CLD, and as the disease progresses, the amount of fibrotic tissue also expands [51,52]. On the other hand, LCL represents functional alterations when CLD progress, making it clear that liver clearance decreases with increasing liver fibrosis. This finding can be explained on a molecular level—99mTc-mebrofenin is an iminodiacetic acid derivate, a lidocaine analog, which is taken up by hepatocytes from the blood through organic anion transporting polypeptide (OATP) receptors on the cell membrane, and excreted into bile canaliculi without any metabolism [38,53]. During the course of CLD, hepatocytes undergo structural alterations, while, together with other changes, the number of OATP receptors decreases; in turn, the uptake of iminodiacetic acid derivates, such as mebrofenin, is also decreased [54,55].

Second, in comparing 2D-SWE and dynamic liver scintigraphy with 99mTc-mebrofenin, we found no significant difference in AUROC at any of liver fibrosis stages (see Figures 3–5), although the numerical value of the area under ROC curve was somewhat higher for liver stiffness in mild and significant fibrosis. On the other hand, in liver cirrhosis, AUROC was higher for liver clearance. These findings support dynamic liver scintigraphy with 99mTc-mebrofenin as a non-inferior imaging method for stratifying CLD.

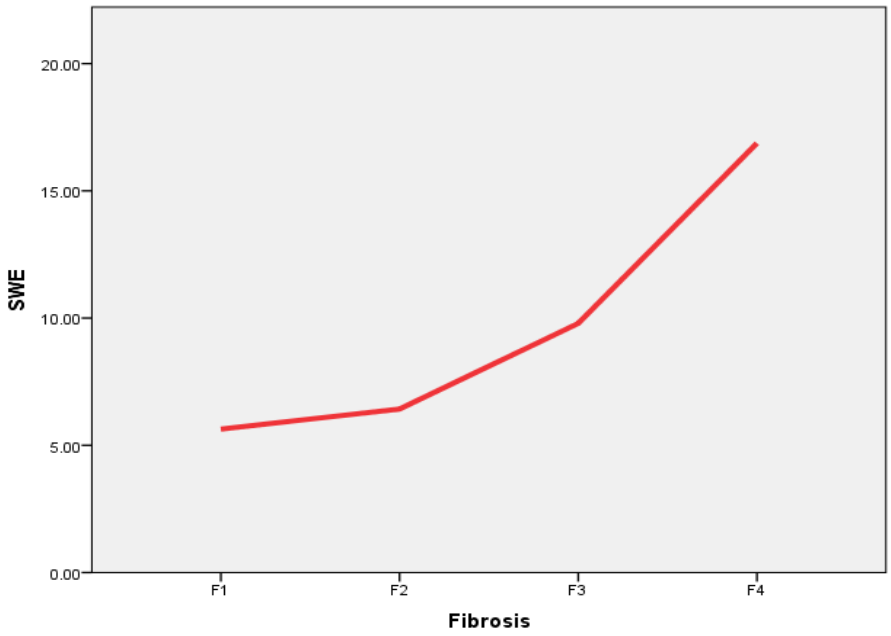


**Figure 7.** The 2D-SWE correlation with increasing liver fibrosis stage. Direct positive association is seen between liver fibrosis stage according to METAVIR and liver stiffness (2D-SWE), measured in kPa. SWE—2D-SWE value represented in kPa; Fibrosis—liver fibrosis evaluated in liver biopsy specimens according to METAVIR.

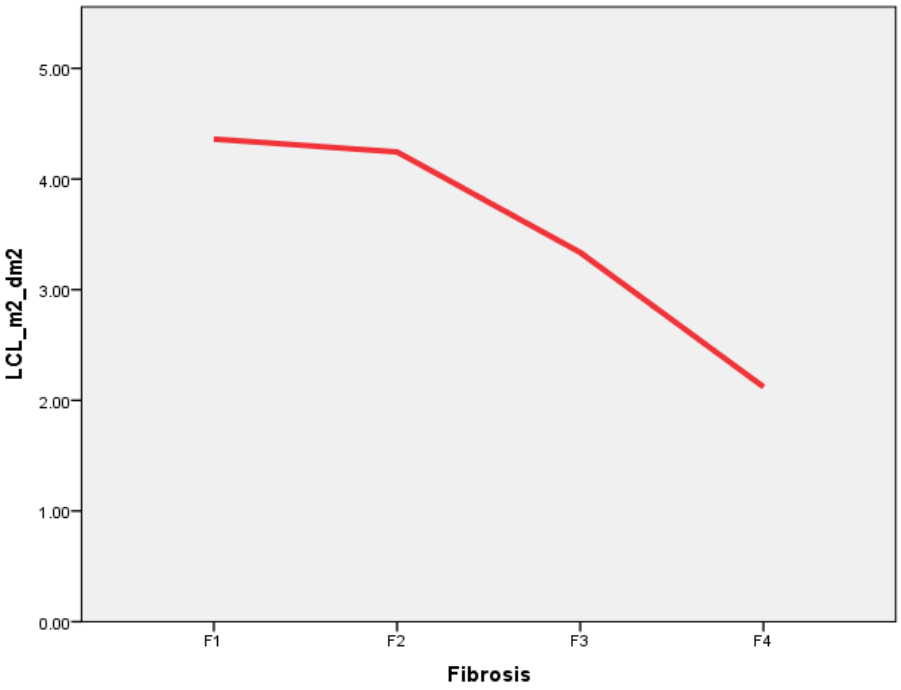


**Figure 8.** Liver clearance (LCL) relation to increasing liver fibrosis stage. Direct negative association between liver clearance (measured in %/min/$m^2$/$dm^2$), and liver fibrosis stage measured according to METAVIR is present. LCL_$m^2$_$dm^2$—liver clearance measured in right liver lobe and corrected with BSA and LA; Fibrosis—liver fibrosis evaluated in liver biopsy specimen according to METAVIR.

Third, both imaging methods work by somewhat different mechanisms—2D-SWE represents mechanical changes in the liver tissue by evaluating the speed of transverse soundwaves propagating in altered hepatic parenchyma [29,30]. A different approach is employed in dynamic liver scintigraphy with 99mTc- mebrofenin. The passage of the iminodiacetic acid derivate mebrofenin through OATP receptors situated on the hepato-

cyte basolateral membrane resembles liver cell function, which is altered as liver fibrosis progresses [53,54]. By referring a different approach to these quantitative liver imaging modalities, we also combined them together to check if there is additional value. Although no additional value was seen in mild and significant fibrosis, at the late stages of CLD (liver cirrhosis), the area under the ROC curve increased from 0.91 to 0.98 (see Figure 6), which signifies an increased accuracy when two imaging modalities are combined.

Several drawbacks and issues of the present study are relevant. This was a single-center, non-blinded study. Its relatively small sample size may hamper a deeper investigation of our study results, especially in some subgroups with particularly small sizes. In addition, the diversity of CLD etiology, including both HBV and HCV patients, as well as some with HIV infections, may pose additional conflict in interpreting results.

The reference standard liver biopsy has its well-known limitations, adding that it does not represent the heterogeneity of liver fibrosis, especially when compared to quantitative imaging, where larger areas of the liver parenchyma are sampled—relying on liver biopsy by itself could be erroneous.

Both imaging and liver biopsy were performed by a single operator, posing potential bias and precluding a comparison of interobserver agreement.

All imaging measurements were performed on a small area of the right liver lobe, which hindered the evaluation of larger volumes and overcoming the possibility of tissue heterogeneity.

## 5. Conclusions

To conclude, our study results showed that both 2D-SWE and dynamic liver scintigraphy with 99mTc-mebrofenin can stage liver fibrosis. We want to emphasize that according to our results, we found no statistically significant differences between these tests. On the contrary, we found that by leaning on the different mechanisms used by these imaging approaches, they can be combined to increase diagnostic accuracy, as we have demonstrated, in the late stages of liver fibrosis.

Indeed, this should be clarified in a wider and multicenter manner, although our preliminary results do look promising.

**Author Contributions:** D.J.—Analyzed and interpreted patient data, performed both imaging studies and liver biopsy procedures, was a major contributor in writing the manuscript. K.M.—Analyzed patient data. D.V., A.E.T., S.J., A.S., K.S., K.M.—read and corrected the manuscript. S.J.—analyzed histological data. All authors have read and agreed to the published version of the manuscript.

**Funding:** This research received no external funding.

**Institutional Review Board Statement:** This study was approved by the Vilnius Regional Biomedical Research Ethics Committee (registered 13/12/2016, reg. no. 158200-16-877-386).

**Informed Consent Statement:** Informed consent was obtained from all subjects involved in the study.

**Data Availability Statement:** The datasets used and/or analyzed during the current study are available from the corresponding author upon reasonable request.

**Conflicts of Interest:** The authors declare that they have no competing interests.

## Abbreviations

| | |
|---|---|
| 2D-SWE | two-dimensional shear wave elastography |
| 99mTc | metastable nuclear isomer of technetium-99 |
| ANOVA | a one-way analysis of variance |
| AUROC | area under receiver operator characteristics curve |
| BMI | body mass index |
| BSA | body surface area |
| CLD | chronic liver disease |
| CT | computed tomography |

| | |
|---|---|
| Gd-EOB-DTPA | gadolinium ethoxybenzyl diethylenetriaminepentaacetic acid |
| HBV | hepatitis B virus |
| HCV | hepatitis C virus |
| HIV | human immunodeficiency virus |
| kPa | kilopascal |
| LA | liver area |
| LCL | liver clearance |
| LEHR | low energy high resolution |
| METAVIR | meta-analysis of histological data in viral hepatitis |
| MRE | magnetic resonance elastography |
| MRI | magnetic resonance imaging |
| mRNA | messenger ribonucleic acid |
| NAFLD | nonalcoholic fatty liver disease |
| NASH | nonalcoholic steatohepatitis |
| OATP | organic anion transporter polypeptide |
| pSWE | point shear wave elastography |
| ROC | receiver operator characteristics curve |
| ROI | region of interest |
| SPECT | single photon emission computed tomography |
| TE | transient elastography |
| USE | ultrasound elastography |

## References


1. Pimpin, L.; Cortez-Pinto, H.; Negro, F.; Corbould, E.; Lazarus, J.V.; Webber, L.; Sheron, N.; The Members of the EASL HEPAHEALTH Steering Committee. Burden of liver disease in Europe: Epidemiology and analysis of risk factors to identify prevention policies. *J. Hepatol.* **2018**, *69*, 718–735. [CrossRef] [PubMed]
2. Cheemerla, S.; Balakrishnan, M. Global Epidemiology of Chronic Liver Disease. *Clin. Liver Dis.* **2021**, *17*, 365–370. [CrossRef] [PubMed]
3. Moon, A.M.; Singal, A.G.; Tapper, E.B. Contemporary Epidemiology of Chronic Liver Disease and Cirrhosis. *Clin. Gastroenterol. Hepatol.* **2020**, *18*, 2650–2666. [CrossRef] [PubMed]
4. World Health Organization. Global Progress Report on HIV, Viral Hepatitis and Sexually Transmitted Infections, 2021: Accountability for the Global Health Sector Strategies 2016–2021: Actions for Impact. Published online. 2021. Available online: https://www.who.int/publications/i/item/9789240027077 (accessed on 14 February 2023).
5. Rockey, D.C.; Bell, P.D.; Hill, J.A. Fibrosis—A Common Pathway to Organ Injury and Failure. *N. Engl. J. Med.* **2015**, *372*, 1138–1149. [CrossRef]
6. Roehlen, N.; Crouchet, E.; Baumert, T.F. Liver Fibrosis: Mechanistic Concepts and Therapeutic Perspectives. *Cells* **2020**, *9*, 875. [CrossRef]
7. Elpek, G.Ö. Cellular and molecular mechanisms in the pathogenesis of liver fibrosis: An update. *World J. Gastroenterol.* **2014**, *20*, 7260–7276. [CrossRef]
8. Zhou, W.-C.; Zhang, Q.B.; Qiao, L. Pathogenesis of liver cirrhosis. *World J. Gastroenterol.* **2014**, *20*, 7312–7324. [CrossRef]
9. Shipley, L.C.; Axley, P.D.; Singal, A.K. Fibrosis del hígado: Una actualización clínica. *Rev. Médica Eur. Hepatol.* **2019**, *7*, 105–117.
10. Fauci, A.; Hauser, S.; Dan Longo, L. *HARRISON'S Gastroenterology and Hepatology*; McGraw Hill: New York, NY, USA.
11. Schuppan, D.; Afdhal, N.H. Seminar Liver cirrhosis. *Lancet* **2008**, *371*, 838–851. [CrossRef]
12. Wang, L.; Wang, M.; Zhao, W.; Shi, Y.; Sun, Y.; Wu, X.; You, H.; Jia, J. Key points of 2015 EASL-ALEH clinical practice guidelines: Non invasive tests for evaluation of liver severity and prognosis. *Zhonghua Gan Zang Bing Za Zhi* **2015**, *23*, 488–492.
13. Tapper, E.B.; Lok, A.S.-F. Use of Liver Imaging and Biopsy in Clinical Practice. *N. Engl. J. Med.* **2017**, *377*, 756–768. [CrossRef] [PubMed]
14. Mendes, L.C.; Stucchi, R.S.; Vigani, A.G. Diagnosis and staging of fibrosis in patients with chronic hepatitis C: Comparison and critical overview of current strategies. *Hepatic Med. Évid. Res.* **2018**, *10*, 13–22. [CrossRef] [PubMed]
15. Berzigotti, A.; Tsochatzis, E.; Boursier, J.; Castera, L.; Cazzagon, N.; Friedrich-Rust, M.; Petta, S.; Thiele, M. EASL Clinical Practice Guidelines on non-invasive tests for evaluation of liver disease severity and prognosis–2021 update. *J. Hepatol.* **2021**, *75*, 659–689. [CrossRef] [PubMed]
16. Dietrich, C.F.; Bamber, J.; Berzigotti, A.; Bota, S.; Cantisani, V.; Castera, L.; Cosgrove, D.; Ferraioli, G.; Friedrich-Rust, M.; Gilja, O.H.; et al. EFSUMB Guidelines and Recommendations on the Clinical Use of Liver Ultrasound Elastography, Update 2017 (Long Version). *Ultraschall der Med.-Eur. J. Ultrasound* **2017**, *38*, e16–e47. [CrossRef]
17. Chin, J.L.; Pavlides, M.; Moolla, A.; Ryan, J.D. Non-invasive Markers of Liver Fibrosis: Adjuncts or Alternatives to Liver Biopsy? *Front. Pharmacol.* **2016**, *7*, 159. [CrossRef]
18. Smith, A.D.; Porter, K.K.; Elkassem, A.A.; Sanyal, R.; Lockhart, M.E. Current Imaging Techniques for Noninvasive Staging of Hepatic Fibrosis. *Am. J. Roentgenol.* **2019**, *213*, 77–89. [CrossRef]

19. Luo, Q.-T.; Zhu, Q.; Zong, X.-D.; Li, M.-K.; Yu, H.-S.; Jiang, C.-Y.; Liao, X. Diagnostic Performance of Transient Elastography Versus Two-Dimensional Shear Wave Elastography for Liver Fibrosis in Chronic Viral Hepatitis: Direct Comparison and a Meta-Analysis. *BioMed. Res. Int.* **2022**, *2022*, 1960244. [CrossRef]
20. Ferraioli, G.; Wong, V.W.-S.; Castera, L.; Berzigotti, A.; Sporea, I.; Dietrich, C.F.; Choi, B.I.; Wilson, S.R.; Kudo, M.; Barr, R.G. Liver Ultrasound Elastography: An Update to the World Federation for Ultrasound in Medicine and Biology Guidelines and Recommendations. *Ultrasound Med. Biol.* **2018**, *44*, 2419–2440. [CrossRef]
21. Panel, A.H.G. Hepatitis C guidance: AASLD-IDSA recommendations for testing, managing, and treating adults infected with hepatitis C virus. *Hepatology* **2015**, *62*, 932–954. [CrossRef]
22. Terrault, N.A.; Lok, A.S.F.; McMahon, B.J.; Chang, K.-M.; Hwang, J.P.; Jonas, M.M.; Brown, R.S., Jr.; Bzowej, N.H.; Wong, J.B. Update on prevention, diagnosis, and treatment of chronic hepatitis B: AASLD 2018 hepatitis B guidance. *Hepatology* **2018**, *67*, 1560–1599. [CrossRef]
23. Chalasani, N.; Younossi, Z.; LaVine, J.E.; Charlton, M.; Cusi, K.; Rinella, M.; Harrison, S.A.; Brunt, E.M.; Sanyal, A.J. The diagnosis and management of nonalcoholic fatty liver disease: Practice guidance from the American Association for the Study of Liver Diseases. *Hepatology* **2018**, *67*, 328–357. [CrossRef] [PubMed]
24. Barr, R.G.; Wilson, S.R.; Rubens, D.; Garcia-Tsao, G.; Ferraioli, G. Update to the Society of Radiologists in Ultrasound Liver Elastography Consensus Statement. *Radiology* **2020**, *296*, 263–274. [CrossRef] [PubMed]
25. Pickhardt, P.J.; Malecki, K.; Kloke, J.; Lubner, M.G. Accuracy of Liver Surface Nodularity Quantification on MDCT as a Noninvasive Biomarker for Staging Hepatic Fibrosis. *Am. J. Roentgenol.* **2016**, *207*, 1194–1199. [CrossRef] [PubMed]
26. Smith, A.D.; Branch, C.R.; Zand, K.; Subramony, C.; Zhang, H.; Thaggard, K.; Hosch, R.; Bryan, J.; Vasanji, A.; Griswold, M.; et al. Liver Surface Nodularity Quantification from Routine CT Images as a Biomarker for Detection and Evaluation of Cirrhosis. *Radiology* **2016**, *280*, 771–781. [CrossRef] [PubMed]
27. Wang, J.-C.; Fu, R.; Tao, X.-W.; Mao, Y.-F.; Wang, F.; Zhang, Z.-C.; Yu, W.-W.; Chen, J.; He, J.; Sun, B.-C. A radiomics-based model on non-contrast CT for predicting cirrhosis: Make the most of image data. *Biomark. Res.* **2020**, *8*, 47. [CrossRef]
28. Huber, A.T.; Ebner, L.; Heverhagen, J.; Christe, A. State-of-the-art imaging of liver fibrosis and cirrhosis: A comprehensive review of current applications and future perspectives. *Eur. J. Radiol. Open* **2015**, *2*, 90–100. [CrossRef]
29. Tang, A.; Cloutier, G.; Szeverenyi, N.M.; Sirlin, C.B. Ultrasound Elastography and MR Elastography for Assessing Liver Fibrosis: Part 1, Principles and Techniques. *Am. J. Roentgenol.* **2015**, *205*, 22–32. [CrossRef]
30. Tang, A.; Cloutier, G.; Szeverenyi, N.M.; Sirlin, C.B. Ultrasound Elastography and MR Elastography for Assessing Liver Fibrosis: Part 2, Diagnostic Performance, Confounders, and Future Directions. *Am. J. Roentgenol.* **2015**, *205*, 33–40. [CrossRef]
31. Pickhardt, P.J.; Graffy, P.M.; Said, A.; Jones, D.; Welsh, B.; Zea, R.; Lubner, M.G. Multiparametric CT for Noninvasive Staging of Hepatitis C Virus–Related Liver Fibrosis: Correlation With the Histopathologic Fibrosis Score. *Am. J. Roentgenol.* **2019**, *212*, 547–553. [CrossRef]
32. Luthra, K.; Galge, A.; Lele, V. Radionuclide methods for evaluation of chronic liver disease—A comparison between colloid & hepatobiliary scans. *J. Nucl. Med.* **2007**, *48* (Suppl. S2), 176. Available online: http://jnm.snmjournals.org/content/48/supplement_2/176P.4.abstract (accessed on 14 February 2023).
33. Li, S.; Sun, X.; Chen, M.; Ying, Z.; Wan, Y.; Pi, L.; Ren, B.; Cao, Q. Liver Fibrosis Conventional and Molecular Imaging Diagnosis Update. *J. Liver* **2019**, *8*, 1–10. [CrossRef]
34. de Graaf, W.; Bennink, R.J.; Veteläinen, R.; van Gulik, T.M. Nuclear Imaging Techniques for the Assessment of Hepatic Function in Liver Surgery and Transplantation. *J. Nucl. Med.* **2010**, *51*, 742–752. [CrossRef] [PubMed]
35. Iguchi, T.; Sato, S.; Kouno, Y.; Okumura, Y.; Akaki, S.; Tsuda, T.; Kobayashi, K.; Kanazawa, S.; Hiraki, Y. Comparison of Tc-99m-GSA scintigraphy with hepatic fibrosis and regeneration in patients with hepatectomy. *Ann. Nucl. Med.* **2003**, *17*, 227–233. [CrossRef] [PubMed]
36. Geisel, D.; Lüdemann, L.; Fröling, V.; Malinowski, M.; Stockmann, M.; Baron, A.; Gebauer, B.; Seehofer, D.; Prasad, V.; Denecke, T. Imaging-based evaluation of liver function: Comparison of $^{99}$mTc-mebrofenin hepatobiliary scintigraphy and Gd-EOB-DTPA-enhanced MRI. *Eur Radiol.* **2015**, *25*, 1384–1391. [CrossRef]
37. de Graaf, W.; van Lienden, K.P.; van Gulik, T.M.; Bennink, R.J. $^{99m}$Tc-Mebrofenin Hepatobiliary Scintigraphy with SPECT for the Assessment of Hepatic Function and Liver Functional Volume Before Partial Hepatectomy. *J. Nucl. Med.* **2010**, *51*, 229–236. [CrossRef]
38. Rassam, F.; Olthof, P.B.; Richardson, H.; van Gulik, T.M.; Bennink, R.J. Practical guidelines for the use of technetium-99m mebrofenin hepatobiliary scintigraphy in the quantitative assessment of liver function. *Nucl. Med. Commun.* **2019**, *40*, 297–307. [CrossRef]
39. Jocius, D.; Vajauskas, D.; Mikelis, K.; Jokubauskiene, S.; Jakutiene, J.; Strupas, K.; Tamosiunas, A.E. Quantitative Assessment of Liver Impairment in Chronic Viral Hepatitis with [$^{99m}$Tc]Tc-Mebrofenin: A Noninvasive Attempt to Stage Viral Hepatitis-Associated Liver Fibrosis. *Medicina* **2022**, *58*, 1333. [CrossRef]
40. Ekman, M.; Fjälling, M.; Friman, S.; Carlson, S.; Volkmann, R. Liver uptake function measured by IODIDA clearance rate in liver transplant patients and healthy volunteers. *Nucl. Med. Commun.* **1996**, *17*, 235–242. [CrossRef]
41. Delong, E.R.; Delong, D.M.; Clarke-Pearson, D.L. Comparing the Areas under Two or More Correlated Receiver Operating Characteristic Curves: A Nonparametric Approach. *Biometrics* **1988**, *44*, 837–845. [CrossRef]

42. Roldán-Nofuentes, J.A. Compbdt: An R program to compare two binary diagnostic tests subject to a paired design. *BMC Med. Res. Methodol.* **2020**, *20*, 143. [CrossRef]
43. Hajian-Tilaki, K. Sample size estimation in diagnostic test studies of biomedical informatics. *J. Biomed. Inform.* **2014**, *48*, 193–204. [CrossRef]
44. Anteby, R.; Klang, E.; Horesh, N.; Nachmany, I.; Shimon, O.; Barash, Y.; Kopylov, U.; Soffer, S. Deep learning for noninvasive liver fibrosis classification: A systematic review. *Liver Int.* **2021**, *41*, 2269–2278. [CrossRef] [PubMed]
45. Gibriel, A.A.; Ismail, M.F.; Sleem, H.; Zayed, N.; Yosry, A.; El-Nahaas, S.M.; Shehata, N.I. Diagnosis and staging of HCV associated fibrosis, cirrhosis and hepatocellular carcinoma with target identification for miR-650, 552–553p, 676–3p, 512–515p and 147b. *Cancer Biomark.* **2022**, *34*, 413–430. [CrossRef] [PubMed]
46. Hagström, H.; Talbäck, M.; Andreasson, A.; Walldius, G.; Hammar, N. Ability of Noninvasive Scoring Systems to Identify Individuals in the Population at Risk for Severe Liver Disease. *Gastroenterology* **2020**, *158*, 200–214. [CrossRef] [PubMed]
47. De Graaf, W.; Van Lienden, K.P.; Dinant, S.; Roelofs, J.; Busch, O.R.C.; Gouma, D.J.; Bennink, R.J.; Van Gulik, T.M. Assessment of Future Remnant Liver Function Using Hepatobiliary Scintigraphy in Patients Undergoing Major Liver Resection. *J. Gastrointest. Surg.* **2009**, *14*, 369–378. [CrossRef]
48. Gupta, M.; Choudhury, P.; Singh, S.; Hazarika, D. Liver functional volumetry by Tc-99m mebrofenin hepatobiliary scintigraphy before major liver resection: A game changer. *Indian J. Nucl. Med.* **2018**, *33*, 277–283. [CrossRef]
49. Olthof, P.B.; Tomassini, F.; Huespe, P.E.; Truant, S.; Pruvot, F.-R.; Troisi, R.I.; Castro-Benitez, C.; Schadde, E.; Axelsson, R.; Sparrelid, E.; et al. Hepatobiliary scintigraphy to evaluate liver function in associating liver partition and portal vein ligation for staged hepatectomy: Liver volume overestimates liver function. *Surgery* **2017**, *162*, 775–783. [CrossRef]
50. Cieslak, K.P.; Bennink, R.J.; de Graaf, W.; van Lienden, K.P.; Besselink, M.G.; Busch, O.R.; Gouma, D.J.; van Gulik, T.M. Measurement of liver function using hepatobiliary scintigraphy improves risk assessment in patients undergoing major liver resection. *HPB* **2016**, *18*, 773–780. [CrossRef]
51. Babu, A.S.; Wells, M.L.; Teytelboym, O.M.; Mackey, J.E.; Miller, F.H.; Yeh, B.M.; Ehman, R.L.; Venkatesh, S.K. Elastography in Chronic Liver Disease: Modalities, Techniques, Limitations, and Future Directions. *Radiographics* **2016**, *36*, 1987–2006. [CrossRef]
52. Heyens, L.J.M.; Busschots, D.; Koek, G.H.; Robaeys, G.; Francque, S. Liver Fibrosis in Non-alcoholic Fatty Liver Disease: From Liver Biopsy to Non-invasive Biomarkers in Diagnosis and Treatment. *Front. Med.* **2021**, *8*, 615978. [CrossRef]
53. de Graaf, W.; Häusler, S.; Heger, M.; van Ginhoven, T.M.; van Cappellen, G.; Bennink, R.J.; Kullak-Ublick, G.A.; Hesselmann, R.; van Gulik, T.M.; Stieger, B. Transporters involved in the hepatic uptake of 99mTc-mebrofenin and indocyanine green. *J. Hepatol.* **2011**, *54*, 738–745. [CrossRef] [PubMed]
54. Bs, A.A.-R.; Roda, G.; Fogueri, U.; Kiser, J.J.; Joy, M.S. Effect of Disease Pathologies on Transporter Expression and Function. *J. Clin. Pharmacol.* **2016**, *56*, S205–S221. [CrossRef]
55. Wang, L.; Collins, C.; Kelly, E.J.; Chu, X.; Ray, A.S.; Salphati, L.; Xiao, G.; Lee, C.; Lai, Y.; Liao, M.; et al. Transporter Expression in Liver Tissue from Subjects with Alcoholic or Hepatitis C Cirrhosis Quantified by Targeted Quantitative Proteomics. *Drug Metab. Dispos.* **2016**, *44*, 1752–1758. [CrossRef] [PubMed]